COMPARISON OF CONVECTION PARAMETERIZATIONS IN AN ATMOSPHERIC GENERAL CIRCULATION MODEL

Zhao-Xin LI

Laboratoire de Météorologie Dynamique du CNRS,
Ecole Normale Supérieure, 24 rue Lhomond, 75231 Paris cedex 05, France

1. Introduction

Atmospheric convection plays an important role in maintaining the equilibrium of energy and water in the climate system through the processes of condensation, latent heat release and vertical redistribution of energy and water. It is accompanied at the same time with complex cloud systems which influence the atmospheric circulation through interaction with radiation. Convection also contributes to the vertical mixing of other constituents in the atmosphere, such as aerosols. However the explicit representation of convection in climate models is practically impossible, since it is mainly a subgrid scale process with horizontal extension of only a few kilometers for an individual cumulus, while climate models have horizontal resolution of a few hundreds kilometers. Thus convection parameterization schemes seek to express the integrated effect of these subgrid scale processes on explicitly resolved large-scale fields.

The first convection scheme used in a General Circulation Model (GCM), which was developed by Manabe et al. (1965), is a moist adjustment procedure for eliminating conditional instability when saturation occurs. This method, referred to as the moist adjustment scheme, was largely used in different GCMs. The scheme of Betts and Miller (1986) is a modified adjustment scheme which allows the relative humidity of the final state to be controlled and provides a time scale for the adjustment. In these adjustment schemes, there is no explicit cloud model to treat the cumulus effects on the large-scale environment. The scheme developed by Kuo (1965, 1974) takes into account large-scale water vapour convergence and evaporation from the surface. These quantities are then considered as the convection forcing to enable the vertical mixing of energy and water. Like the moist adjustment procedure, the Kuo scheme does not have any explicit cloud model.

Another category of convection parameterization, called "mass flux schemes", concerns more comprehensive cumulus convection schemes since they attempt to parameterize explicitly the upward and downward fluxes in the convective tower and the induced motions in the environmental air. The most popular one is that of Arakawa and Schubert (1974). They introduced the concept of cumulus clouds ensemble and considered a spectrum of cloud types connected with the environment through mass fluxes in the clouds and detrainment of cloud air at the top of every cumulus tower. Many convection schemes developed recently (Emanuel 1991; Hack 1994) belong to this category.

The scheme proposed by Tiedtke (1989) is a simple mass flux convection scheme. The ensemble model of clouds is not used, but instead a bulk cloud model. Only one convective tower is considered where the entrainment and detrainment between the cloud tower and the environment can take place at any number of levels between the free convection level and the free sinking level. The free sinking level is of course lowered by the entrainment and detrainment processes. The convection closure is realized through the large-scale moisture convergence.

Presently, parameterization of convection in large-scale models is still in a developing stage and the problems associated with the closure and the cloud model raise many on-going studies (Arakawa 1994; Emanuel et al. 1994). It is important to intensely compare different numerical schemes and their performance in climate simulations. In this paper, we use a GCM developed at the Laboratoire de Météorologie Dynamique (LMD) to compare three convection schemes.

2. Model description

The model used in this study is derived from the LMD standard GCM, first described in Sadourny and Laval (1984). But the code has been rewritten with more physical consistency, and organized in a more flexible manner for utilization. The grid points are regularly distributed in the longitude-latitude coordinates with resolution of 64 longitudes $\times$ 48 latitudes. The model has 11 vertical layers, unevenly spaced to allow a better resolution in the boundary layer. The time step is 6 minutes, however, the contributions of physical parameterization are evaluated only every 30 minutes. We give here a brief description of the physical package used in this paper.

2.a. Boundary layer

In the boundary layer, the turbulent mixing is represented by an eddy diffusivity formulation. To avoid numerical instability, the time stepping procedure is implicit. The exchange coefficients and the drag coefficient over the surface are calculated through a Richardson number-dependent function. When cloud condensation occurs, the Richardson number is interpolated between its dry and moist values.

2.b. Surface model

The surface model is very simple and we consider only a homogeneous layer of 150 mm. The calculation of surface temperature is incorporated in the boundary layer and based on the surface energy balance equation. The thermal capacity of the surface depends on surface nature. For the surface moisture, a simple bulk model is used whose holding capacity is fixed at 150 mm of water, and all the water above this value is lost as runoff. The real evaporation rate is equal to the potential evapotranspiration capacity multiplied by a function of the surface moisture content. Accumulation of snow depends on the rates of snow fall, sublimation and melting. When melting occurs, the surface temperature is modified accordingly.

2.c. Stratiform precipitation and cloud generation scheme

Cloud liquid water is a prognostic variable of the model, which is calculated by considering the different source and sink terms. At present, clouds created by convection are not considered. Only those associated to stratiform condensation are taken into account. The calculation begins at the top of the atmosphere. Rain and snow fluxes are calculated separately from the top of the atmosphere to the surface. Condensation is the source term for both the snow flux and the rain flux. Fractional condensation for a grid point is allowed through a statistical approach. The temperature is assumed constant but the water vapour (q) follows a uniform distribution between $(q - \Delta q)$ and $(q + \Delta q)$. The condensed water (l) is then shared into two parts: one part precipitates as rain or snow (according to the layer temperature), another remains in the atmosphere as cloud liquid or solid water, and is then used in the radiative transfer calculations.

2.d. Radiative transfer

The radiative transfer code has been designed by Fouquart and Bonnel (1980) for the solar radiation and by Morcrette (1991) for the terrestrial radiation. For the time being, the diurnal cycle of insolation is not taken into account. The radiation code is called at every physical time step to calculate the influence of clouds, the clear-sky transmission coefficients being, however, evaluated only every four hours.

2.e. Manabe convection scheme

The Manabe convection scheme (Manabe et al. 1965) adjusts the atmospheric column, when it is conditionally unstable and saturated, to neutrality. The total energy is conserved through the moist adjustment procedure.

Let us consider two levels l_1 and l_2, the moist adjustment procedure is applied when the following conditions hold:

$$dT < -\Gamma_m dz, \tag{1}$$

$$\sum_{l=l_1}^{l=l_2}(q - q_s)dp > 0, \tag{2}$$

where T denotes the temperature, p the pressure, z the vertical height, Γ_m the moist lapse rate of temperature, and q_s the saturated value of water vapour. Any water mass condensed in such a procedure is immediately precipitated.

2.f. Convection scheme used in the standard model of LMD

The standard version of the LMD GCM applies the Kuo (1965) scheme after using the Manabe scheme described above. This is done mainly in order to overcome the defect of the moist adjustment scheme which is not efficient enough to transport water and energy to the upper troposphere. The combined utilization of two convection schemes is a particular character of the LMD GCM and it gives additional possibility for the variation of model climate at different scales.

Let h denote the saturated value of moist static energy and h_b the value of h at the cloud base (l_b). Convection extends to the highest level (l_t) where $h < h_b$, and takes place when

$$\Delta \equiv \sum_{l=l_b}^{l=l_t} \delta_l d\sigma_l > 0, \tag{3}$$

where δ_l is the humidity convergence for layer l and $d\sigma_l$ is the layer thickness. The total quantity of water vapour convergence necessary to make the whole column (between l_b and l_t) saturated and unstable is

$$\Delta_t = \sum_{l=l_b}^{l=l_t}(q_s - q)d\sigma_l + \sum_{l=l_b}^{l=l_t}(h - h_b)d\sigma_l. \tag{4}$$

Suppose that all the water vapour convergence is entirely pumped into the clouds, so the fraction of the mesh occupied by the cumulus is given by Δ/Δ_t. The temperature and water vapour values in the cumulus tower are obtained by the moist adiabatic process while the excess of moisture precipitates. The cumulus tower is then dissipated immediately into the environment, which permits to obtain the final state of the column after convection has occurred.

In the standard version of the LMD model, the value of h_b is obtained by averaging the h values of the third and fourth layers, which means that the convection base is just below the top of the boundary layer, itself consisting of the lowest four layers. This choice seems somewhat arbitrary and we use, in the present study, the free convection level calculated by lifting a surface air parcel to its positive buoyant level.

2.g. Tiedtke convection scheme

The Tiedtke convection scheme is a mass flux parameterization which explicitly takes into account the upward mass flux (M_u) and the downward mass flux (M_d) in the convective tower, as well as the compensating flux in the environment. The scheme is not based on the idea of cloud ensemble but describes the bulk properties of clouds.

The energy flux (F_c) due to convection can be written as:

$$F_c = M_u s_u + M_d s_d - (M_u + M_d)\overline{s}, \tag{5}$$

where s_u is the dry static energy in the updrafts, s_d is the dry static energy in the downdrafts and $\overline{s}$ is the mean value of the environment.

The water vapour flux (Q_c) is:

$$Q_c = M_u q_u + M_d q_d - (M_u + M_d)\overline{q}, \tag{6}$$

where q_u is the humidity in the updrafts, q_d is the humidity in the downdrafts and $\overline{q}$ is the mean value in the environment.

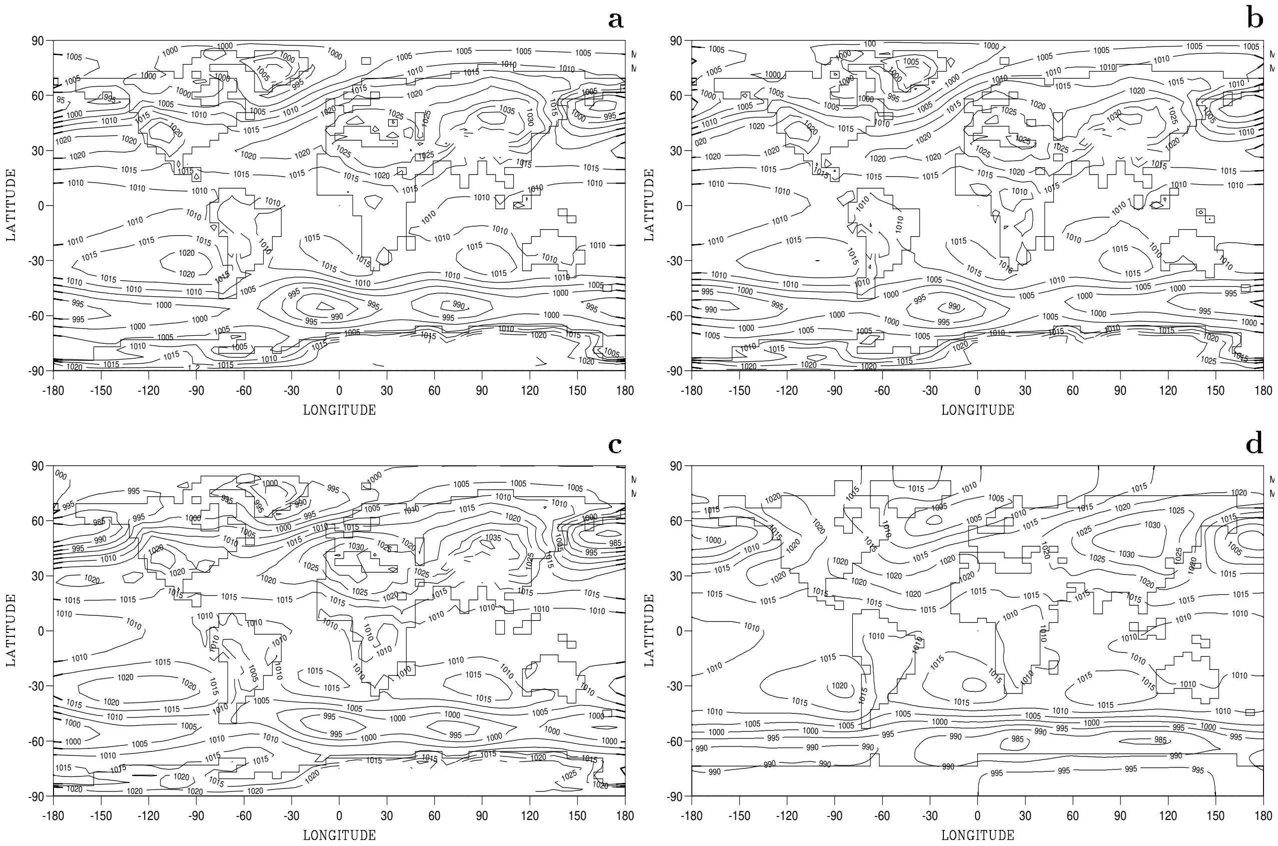

FIG. 1. January sea level pressure (mb): (a) experiment M; (b) experiment L; (c) experiment T; (d) observation compiled by Schutz and Gates (1971, 1972).

These fluxes are determined by the rates of mass entrainment and detrainment of the convection towers through the large-scale convergence and the exchanges at the edges of convection due to turbulence. At the bottom, two closures are considered for penetrative convection and shallow convection: penetrative convection corresponds to a strong convergence of water vapour; shallow convection occurs in the case of presence of an inversion layer over the planetary boundary layer in the sub-tropical regions.

3. RESULTS

We performed 3 experiments corresponding to the 3 convection schemes described above, the rest of the model being kept unchanged. All the experiments have been run for 5.5 years and the results presented in this paper are averages over the last five years. The prescribed sea surface temperature and sea ice distribution are from the AMIP (Atmospheric Model Intercomparison Project) mean data over the period from 1979 to 1988. The monthly mean values are interpolated to daily values to force the atmospheric model. Hereafter, M denotes the experiment with the Manabe convection scheme, L the experiment with the mixed convection scheme of the LMD standard model, and T the experiment with the Tiedtke convection scheme.

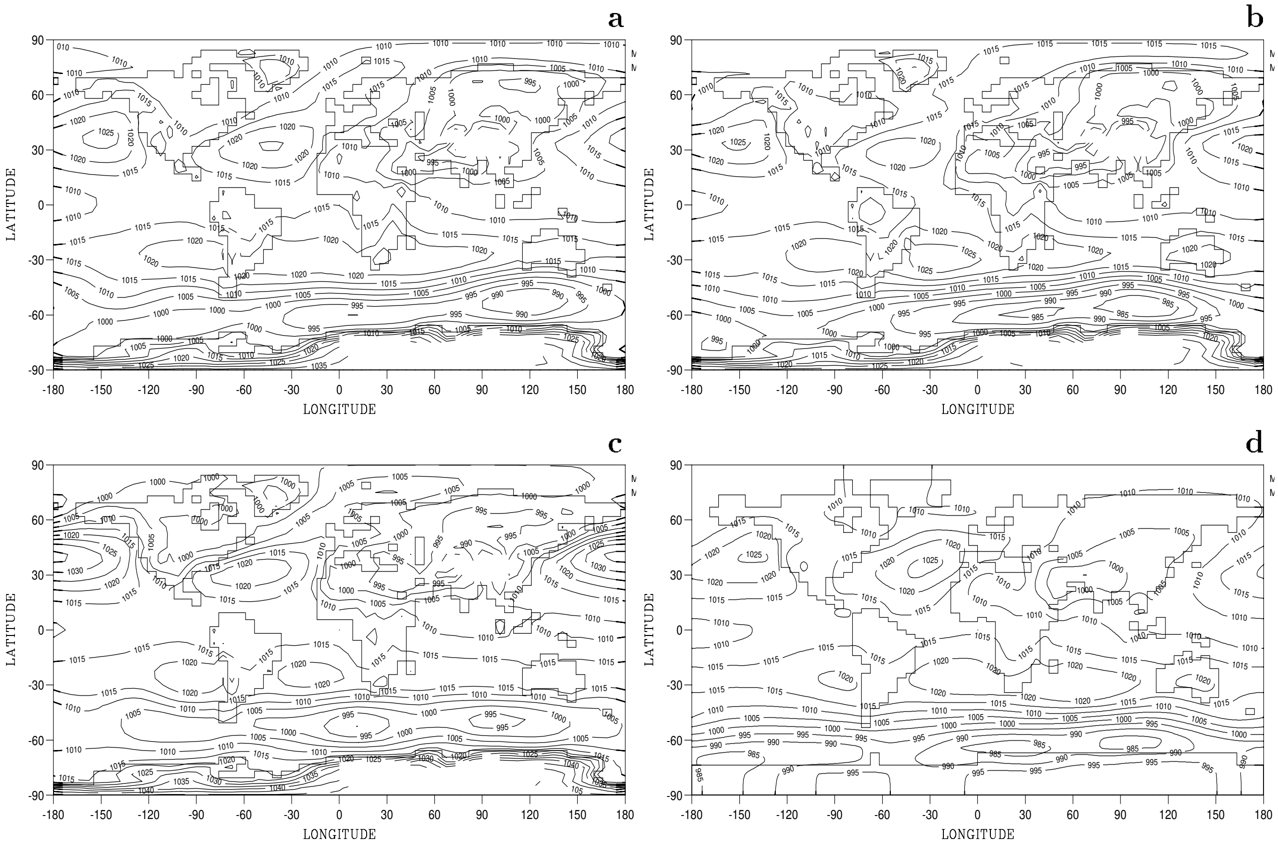

FIG. 2. Same as in Fig. 1, but for July.

3.a. Sea level pressures

Model sea level pressures are calculated from the extrapolation of surface pressures by assuming a hydrostatic balance with a constant temperature taken at the surface. Thus in mountainous regions the pressures are artificial and the extrapolation is rejected when the surface altitude exceeds 2500 m.

The January simulated and observed sea level pressures are plotted in Fig. 1. The observed data were compiled by Schutz and Gates (1971, 1972). All the three experiments capture the main structures of the observed global distribution. The position and the extension axis of the Icelandic and Aleutian lows are well simulated, but the intensity is too strong compared to the observation. The Siberian high is fairly well positioned. All three experiments simulate a high in North America, which is present, but with a larger extension, in the observations. A major shortcoming of the simulations is the anticyclone, located at the Azores with small activity in winter, since this anticyclone is shifted eastwards to the continent and amplified due to the cold land mass. We note that the meridional gradient of the simulated sea level pressure at midlatitudes of the Northern Hemisphere is larger than in the observations. In the Southern Hemisphere, the three summer anticyclones over the oceans are well simulated. The climatological low pressure troughs at lower latitudes over South America and Africa are captured by the

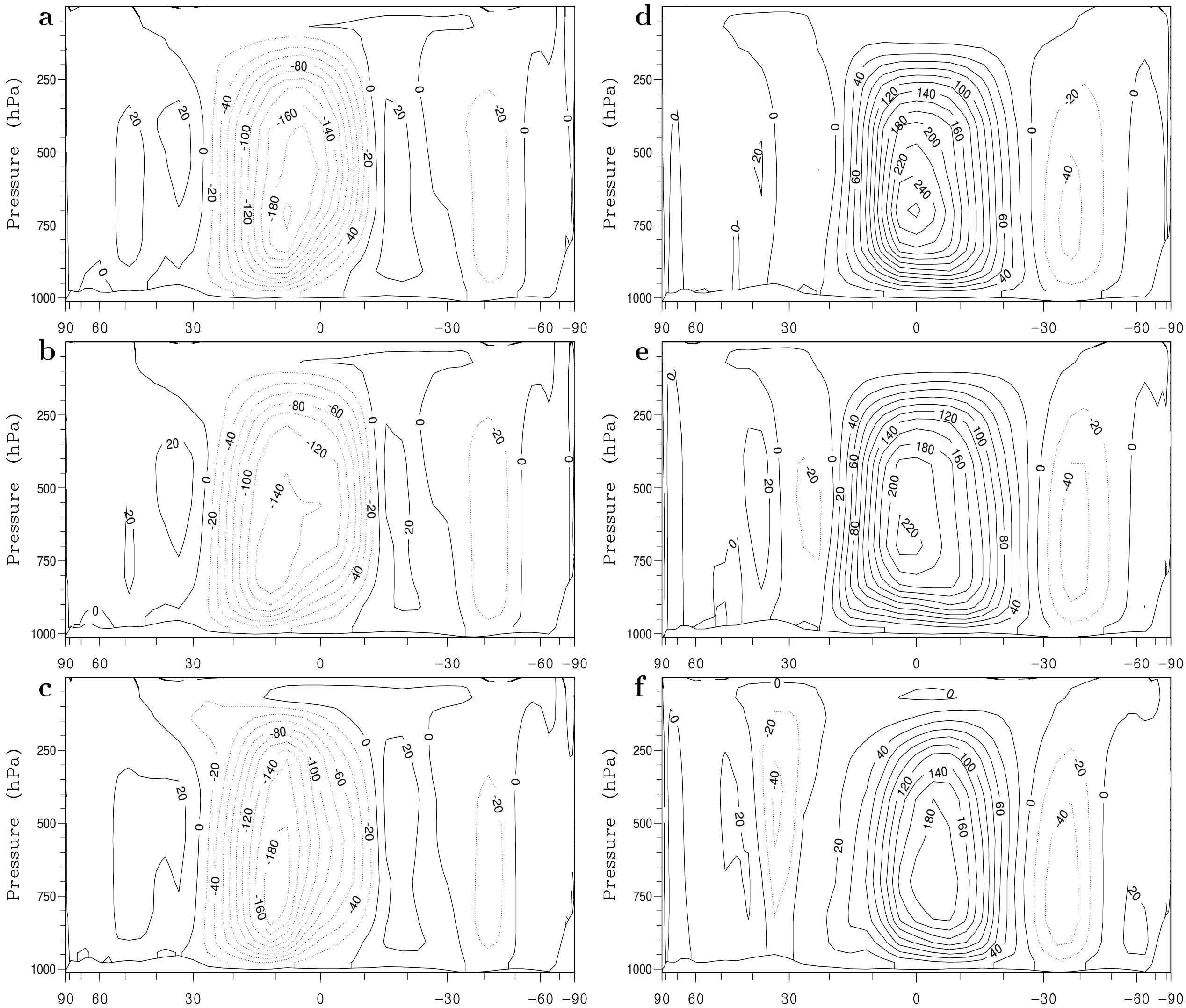

FIG. 3 January (left panel) and July (right panel) meridional mass transport streamfunction (10^9 kg s^{-1}): (a) and (d) for experiment M; (b) and (e) for experiment L; (c) and (f) for experiment T.

model. The Antarctic circumpolar trough of low pressure is not strong enough in the model and the position is also shifted about 10° north of its observed location.

The July simulated and observed sea level pressures are plotted in Fig. 2. In the Northern Hemisphere, two anticyclones are situated over the Pacific and the Atlantic (the Azores), and two thermal lows over North America and the Tibetan Plateau, the latter with a lobe projecting to North Africa. The pattern of the pressure distribution is well simulated compared to the climatology. However, the low pressures over continents seem too strong and the high pressure over the Atlantic not high enough, which is particularly true for experiments L and T where the anticyclone over the Azores is very weak. At 30°S, in the descending branch of the Hadley cell, high sea level pressures are simulated with 4 centers of activity over Australia, the Indian Ocean, the Atlantic and East Pacific. The Antarctic circumpolar trough of low pressure around 60°S is well simulated in all

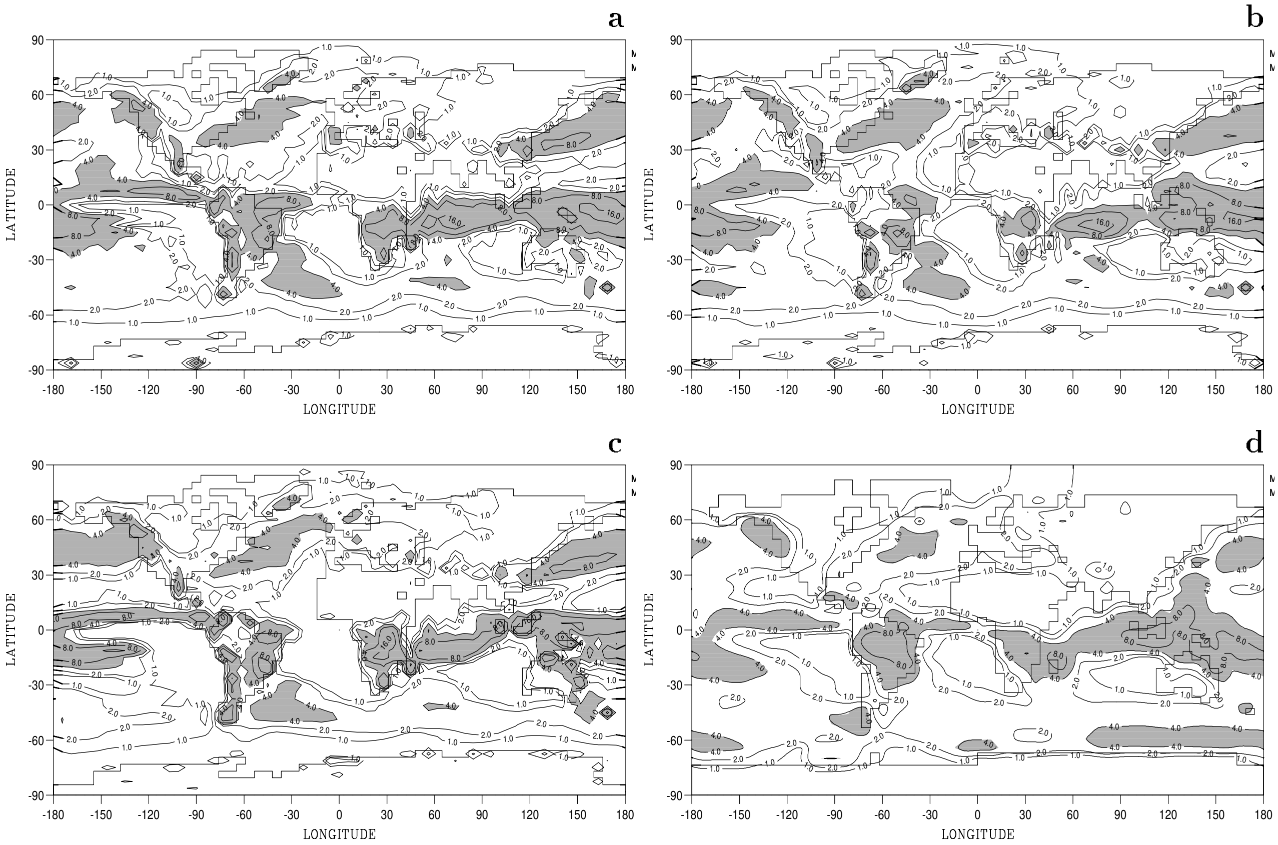

FIG. 4. January precipitation (mm day^{-1}): (a) experiment M; (b) experiment L; (c) experiment T; (d) observation compiled by Jaeger (1976). The contour interval is 1, 2, 4, 8, 16, and 32 mm day^{-1}. Shaded regions exceed 4 mm day^{-1}.

three experiments, although the position is somewhat too much to the north.

3.b. Meridional circulation

Fig. 3 shows the simulated meridional streamfunction, for January and July respectively. It is computed from the mean meridional wind by using the continuity equation. The horizontal axis is plotted in sine of the latitude. For January, the meridional circulation in M is very close to that of experiment T, however, the dominated winter Hadley circulation in L is slower compared to M and T. For July, the figures mainly show the Hadley circulation of the winter hemisphere, but we can recognize the other patterns of the meridional circulation, such as the Ferrel cell in midlatitudes and the polar cell in high latitudes. For both January and July, in the order L, T and M, the intensity of the winter hemisphere Hadley cell increases, but that of the summer hemisphere Hadley cell decreases. In the same order, the intertropical convergence zone is shifted poleward in the summer hemisphere. Compared to the analysed data (not shown here) produced at the European Centre for Medium-range Weather Forecasts (ECMWF), the simulated mean meridional circulation, its geographical position and its seasonal variation are better simulated in experiment T than in the other two experiments.

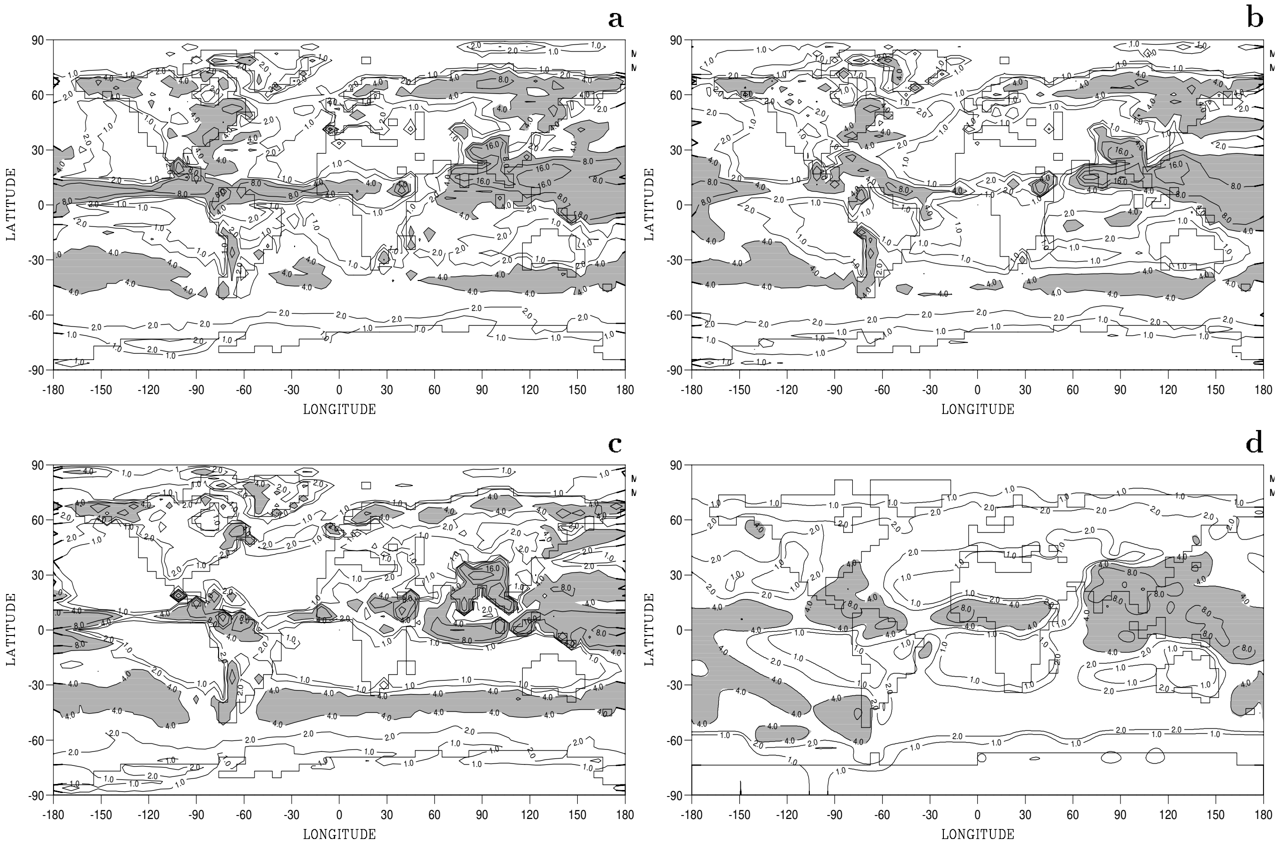

FIG. 5. Same as in Fig. 4, but for July.

3.c. Precipitations

January precipitations are plotted in Fig. 4 for the three simulations and the observation respectively. All three experiments are generally realistic. We can remark, in the Northern Hemisphere, two branches of large precipitation situated over the Atlantic and the Pacific, with lobes projecting respectively into the Mediterranean Sea, North Europe, and into the Northern America continent. In the tropical regions, large precipitations are simulated over Central America, Africa and Indonesia in agreement with the observations. The ITCZ (InterTropical Convergence Zone) over the Atlantic and the Pacific for experiment M and L is very close to observations. However the ITCZ over the Atlantic is not marked in experiment T. The simulated ITCZ over the Western Pacific, for experiment T seems so extend southwards and cover too large regions of North-East Australia. In the midlatitudes of the Southern Hemisphere and for all three experiments, the rain belt related to baroclinic perturbations does not sufficiently extend to the south, which corresponds to the bad position of the Antarctic circumpolar trough for the sea level pressure.

For July (Fig. 5), the position and the intensity of the ITCZ are well simulated in L and T but the ITCZ is too strong in M. The summer monsoon precipitations over India and South-East Asia are also well simulated with very heavy precipitation in all three experiments. Over the Indian Ocean and the Western Pacific, experiment T has a visible structure of double ITCZ but experiments M and L have only one. This feature is probably related to the convection closure assumption used in T, which is based on the large-scale water vapour convergence rate. In the sub-tropical regions of both hemispheres reached by the descending branches of the Hadley cell, we have less precipitation, but these arid areas extend too largely in T compared to the climatology (this is also true for January). However, experiment T gives too much precipitations over Sahara. The midlatitude rain belts of the Southern and Northern Hemispheres are simulated in a correct position, but their intensity seems too strong.

4. Conclusions

We have compared three convection schemes in a low resolution atmospheric GCM. The first scheme is the moist adjustment scheme (Manabe et al. 1965), which does not take into account the subgrid scale phenomena, but just attempts to simulate the integrated effects of convection in order to maintain the model atmosphere in a state of static stability. The second one is a combination of the Manabe scheme and the Kuo (1965) scheme, as used in the standard version of the LMD model. The third one is the mass flux scheme proposed by Tiedtke (1989) which tries to parameterize explicitly the up- and downward mass fluxes in the convective tower.

We examined the sea level presure, the precipitation and the meridional circulation. The climatologies simulated by using the three different convection schemes are different from each other, but they are generally in a reasonable agreement with the observed climatology. From the results, it is difficult to give a preference to one of them. But we have a preference for the Tiedtke scheme since it is a more comprehensive parameterization which allows to refine the microphysical aspects of convection and associated clouds. Furthermore, it is more efficient at transporting water vapour and energy into the upper layers of the atmosphere. However, most models using the Manabe or the Kuo schemes have the deficiency of a too cold and dry troposphere. Further studies will be made in the future to study the influence of convection parameterizations on the model variability at different scales and on the model sensitivity to external perturbations.

Acknowledgments. The author would like to thank Drs. A. Hollingsworth and M. Tiedtke for providing the ECMWF physical package and therefore the convection code. He also thanks Drs. J.-F. Geleyn, K. Laval, H. Le Treut and R. Sadourny for their advice, and Drs. L. Fairhead, F. Hourdin and P. Le Van for their assistance. The author also thanks Drs. J.-F. Royer and O. Talagrand for their comments on an earlier draft. This work was partly supported by PNEDC (French national climate programme) and CEC (Commission of the European Community).

References

Arakawa, A., 1994: Closure assumptions in the cumulus parameterization problem. In Cumulus parameterization (Eds: K. A. Emanuel and D. J. Raymond), Amer. Meteor. Soc., Boston, 1-15.

Arakawa, A., and W. H. Schubert, 1974: Interaction of a cumulus cloud ensemble with the large-scale environment. *J. Atmos. Sci.*, **31**, 674-701.

Betts, A. K., and M. J. Miller, 1986: A new convective adjustment scheme. Part II. Single column tests using GATE wave, BOMEX, ATEX and arctic air-mass data sets. *Quart. J. Roy. Meteor. Soc.*, **112**, 693-709.

Emanuel, K. A., 1991: A scheme for representing cumulus convection in large-scale models. *J. Atmos. Sci.*, **48**, 2313-2335.

Emanuel, K. A., J. D. Neelin, and C. S. Bretherton, 1994: On large-scale circulations in convecting atmospheres. *Quart. J. Roy. Meteor. Soc.*, **120**, 1111-1143.

Fouquart, Y., and B. Bonnel, 1980: Computations of solar heating of the Earth's atmosphere: A new parameterization. *Beitr. Phys. Atmosph.*, **53**, 35-62.

Hack, J. J., 1994: Parameterization of moist convection in the National Center for Atmospheric Research community climate model (CCM2). *J. Geophys. Res.*, **99D**, 5551-5568.

Kuo, H. L., 1965: On formation and intensification of tropical cyclones through latent heat release by cumulus convection. *J. Atmos. Sci.*, **22**, 40-63.

Kuo, H. L., 1974: Further studies of the parameterization of the influence of cumulus convection on large-scale flow. *J. Atmos. Sci.*, **31**, 1232-1240.

Jaeger, L., 1976: Monatskarten des Niederschlags für die ganze Erde. *Ber. Dtsch. Wetterdienstes.*, **18**, No. 139, 38pp.

Manabe, S., J. Smagorinsky, and R. F. Strickler, 1965: Simulated climatology of a general circulation model with a hydrologic cycle. *Mon. Wea. Rev.*, **93**, 769-798.

Morcrette, J.-J., 1991: Radiation and cloud radiative properties in the ECMWF operational weather forecast model. *J. Geophys. Res.*, **96D**, 9121-9132.

Sadourny, R., and K. Laval, 1984: January and July performance of the LMD general circulation model. In *New perspectives in climate modelling*, (Eds.: A. Berger, C. Nicolis), Elsevier, 173-198.

Schutz, C., and W. L. Gates, 1971: Global climatic data for surface, 800 mb, 400 mb: January. R-915-ARPA, pp. 173, Rand - Santa Monica.

Schutz, C., and W. L. Gates, 1972: Global climatic data for surface, 800 mb, 400 mb: July. R-1029-ARPA, pp. 180, Rand - Santa Monica.

Tiedtke, M., 1989: A comprehensive mass flux scheme for cumulus parameterization in large-scale models. *Mon. Wea. Rev.*, **117**, 1779-1800.